This article has been accepted for publication in IEEE Microwave Magazine. This is the author's version which has not been fully edited and content may change prior to final publication. Citation information: DOI 10.1109/MMM.2023.3293617

IEEE Magazine Article

Microwaves See Thin Ice: A Review of Ice and Snow Sensing using Microwave Techniques

A. Shah, O. Niksan, M. C. Jain, K. Colegrave, M. Wagih, M. H. Zarifi**

Authors:

University of British Columbia

Aaryaman Shah

Omid Niksan

Mandeep Char Jain

Keatin Colegrave

Prof. Mohammad H. Zarifi*

University of Glasgow

Dr. Mahmoud Wagih*

Dr. Mahmoud Wagih*
James Watt School of Engineering, University of Glasgow, Glasgow, G12 8QQ, UK
mahmoud.wagih@glasgow.ac.uk

Prof. Mohammad H. Zarifi*
Okanagan Microelectronics and Gigahertz Applications (OMEGA) Lab, School of Engineering, University of British Columbia, Kelowna, BC, V1V 1V7, Canada
mohammad.zarifi@ubc.ca

This article has been accepted for publication in IEEE Microwave Magazine. This is the author's version which has not been fully edited and content may change prior to final publication. Citation information: DOI 10.1109/MMM.2023.3293617

Authors Email Address, ORCID and Affiliations

Name	Email	ORCID	Affiliations
Aaryaman Shah [1]	aaryaman.shah@ubc.ca	0000-0002-4760-4309	Graduate Student Member, IEEE Student Member, SAE
Omid Niksan [1]	omid.niksan@ubc.ca	0000-0002-5586-3423	Graduate Student Member, IEEE
Mandeep Char Jain [1]	mandeepchajerjain@gmail.com	0000-0003-4105-8711	Graduate Student Member, IEEE
Keatin Colegrave [1]	keatin.colegrave@ubc.ca	0000-0001-7903-741X	Graduate Student Member, IEEE
Dr. Mahmoud Wagih [2]	mahmoud.wagih@glasgow.ac.uk	0000-0002-7806-4333	Member, IEEE
Prof. Mohammad H. Zarifi [1]	mohammad.zarifi@ubc.ca	0000-0001-5544-3966	Senior Member, IEEE

[1] Okanagan Microelectronics and Gigahertz Applications (OMEGA) Lab, School of Engineering, The University of British Columbia, Kelowna, BC, V1V 1V7, Canada

[2] James Watt School of Engineering, University of Glasgow, Glasgow, G12 8QQ, UK

This article has been accepted for publication in IEEE Microwave Magazine. This is the author's version which has not been fully edited and content may change prior to final publication. Citation information: DOI 10.1109/MMM.2023.3293617

Ice Sensing: An Ongoing Challenge

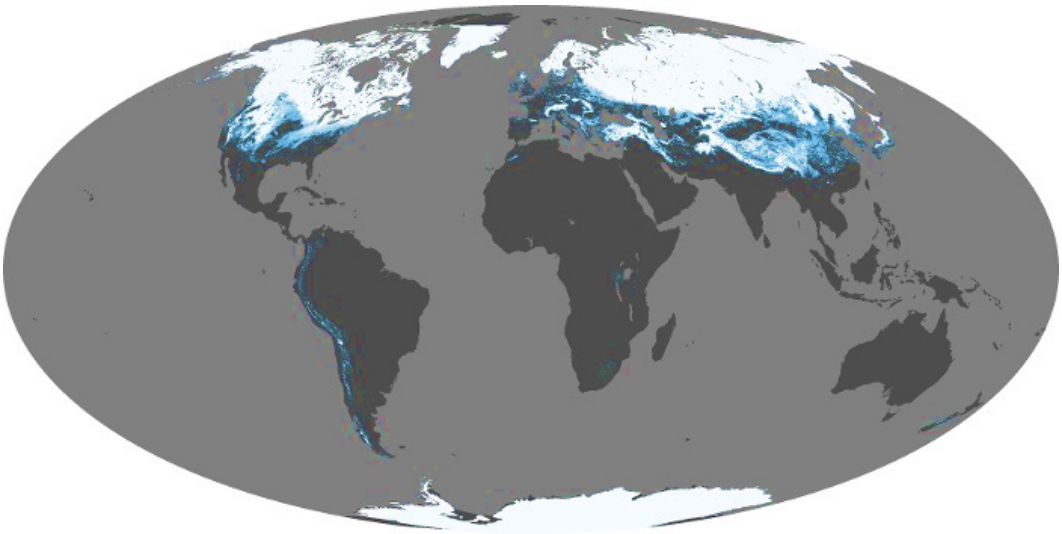

Figure 1: Snow cover in February 2022 obtained by NASA's Terra Satellite [1]

Ice and snow are a reality that a large percent of the global population experience on a regular basis, with over 31% of the earth's landmass [2] experiencing seasonal snow and ice accretion (as shown in Fig. 1, a satellite image of the global snow cover for February 2022) [1]. In the US alone, ice and snow impact 70% of its population, resulting in over 1300 annual deaths from icing related roadway accidents, and causing an estimated 2.3 billion dollars to be spent each year on roadway snow and ice control operations [3]. The infrastructure in regions that receive ice and snow must be specially designed to reliably operate in winter weather conditions, with specific considerations for power grids [4], antenna communication structures, and cable bridges [5]. Expanding marine shipping and industrial operations in arctic regions have increased the need for safe and reliable operation of equipment and ships in atmospheric accretion and salty-icing conditions [6]. Wind turbines with blades rotating at great speeds, heigh up in the air, require thorough design considerations for atmospheric ice formation to prevent damage from icing, which can result in substantial power reduction or complete outage [7]. Similarly, ice accretion on flying objects, such as aircraft wings or turbo-propellors, are highly critical challenges and have been a focus for sensing and de-icing for decades [8] due to the fatal effects of icing on airplanes [9].

For continued operation in icy or snowy conditions, accretion must be accurately sensed in time for stoppage or de-icing. Various commercial technologies [5], [6], [10], [11] and industrial standards [12], [13] for ice detectors exist. These application-specific sensors each apply different technologies, including magnetostrictive vibration [14], capacitive [15], optical [16], [17], and ultrasonic [18], [19] methods for detection of ice or snow. Magnetostrictive sensors, used as primary inflight ice detectors for airplanes [14], offer "global" air condition measurements and result in total airplane de-icing, in place of more optimized targeted "local" ice removal [15]. Commercial wind turbine sensors are also "global" sensors that can be insensitive to the actual onset of icing on the blades and result in late turbine stoppage [11]. Current optical methods for ice detection suffer from real-world noise and are expensive and challenging to integrate [16], [20], [21]. Capacitive and resistive roadway ice sensors have limited accuracy and are high power solutions that require challenging, wired installation [22]. Ultrasonic methods are relatively new [18], and require testing in real-world, high vibration and noise environments. As we move toward greener, more efficient systems, current "global" ice detection and de-icing methods must be improved or replaced with localized ice sensing and "guided" optimal de-icing. This necessary change requires a thorough understanding of the type and contents of the localized ice accretion to efficiently de-ice the application-specific surfaces for reliable operation in harsh winter conditions.

Recent advances in microwave-based sensing methods have exhibited excellent performance as highly accurate real-time sensors for industrial [23], biomedical [24]–[27], and chemical applications [28]–[31]. Microwave devices have been successfully implemented for characterization of materials in solid, liquid, and gaseous phases [32]. These types of microwave sensors are compatible with wireless communication protocols and allow for communication and implementation of wireless sensing mechanisms [33]. These sensors are capable of reliable operation in harsh environments and are easily implemented due to their low fabrication cost. One of the most prominent industrial implementations of microwave sensors is for moisture and humidity sensing in the pulp and wood industry [34]. In addition, microwave flowrate sensors for oil, gas, and water measurements are also commercially available [35]. Microwave sensors see widespread use in wireless downhole monitoring, corrosion monitoring, and subsea oil and gas applications [36]. As biomedical sensors, microwave devices see wide application in non-invasive sensing, diagnostics, and therapy due to the relatively innocuous nature of microwave radiation and its ability to penetrate biological media [37].

Specifically, resonant microwave structures have demonstrated extreme sensitivity, accuracy, and repeatability, as well as high quality-factors [33]. These various attributes make microwave sensors great candidates for further investigation as wireless, low-cost, and low-power sensors for highly accurate, targeted ice and snow detection.

Far-Field Remote Microwave Ice Detection

Microwave technology also enables the remote detection of ice, water, and snow. This is achieved by measuring and differentiating passively generated scattering or actively generated backscattered microwave signals, often referred to as “doppler measurements of echoed signals” or “radiometry” [38]. These techniques have been widely implemented on satellites which conduct various measurements of atmospheric and global phenomena [39]. These instruments allow for large scale measurement of material, like the approximate amount of polar sea ice [40], and are used to monitor climate change related phenomena [41]. Numerous studies, with one of the earliest reported in [42], have been conducted on accurate electromagnetic modeling of ice and snow with C-band radiometry. Similar to RADAR technology, radiometric sensing technology has been constrained by the spatial resolution in ice detection and the power requirements for space-borne missions. In a paper published in 2018, Mousavi et al. demonstrated the feasibility of a passive, low-power system for time-domain measurement of ice and snowpack [43]. This development allowed for ice and snowpack thickness detection as the travel time of microwaves within these mediums of interest was differentiated.

Remote microwave sensing is a very useful implementation of microwave technology for detecting and tracking atmospheric, environmental, and large-scale phenomena. For localized measurement of thin ice accretion at the onset of icing, microwave resonant and wireless structures show far more accurate results and hence are proposed as sensors for real-time detection of ice and snow accretion on surfaces of interest.

This article has been accepted for publication in IEEE Microwave Magazine. This is the author's version which has not been fully edited and content may change prior to final publication. Citation information: DOI 10.1109/MMM.2023.3293617

Fundamental Background

A material's interaction with electromagnetic waves can be characterized by two distinct properties, its degree of polarization or real permittivity, and its dielectric loss or imaginary permittivity [44]. Materials can undergo molecular displacement when exposed to time-harmonic (alternating) electromagnetic fields. Exploiting this phenomenon, the field of microwave sensing differentiates materials based on their interaction with electromagnetic fields [45].

A microwave sensor can be viewed as a *"resonator"* which displays a predictable, characteristic electromagnetic resonance as a function of a structure's geometry and nearby material. These measurable characteristics are highly accurate for optimized structures [46]. When materials are introduced into the sensor's local environment, its resonant characteristics are perturbed [47]. Exploiting this phenomenon, microwave sensor designers detect materials in the vicinity of these resonant structures by characterizing the change in resonant frequency, resonant amplitude, and general frequency response [48].

A thoroughly developed microwave resonator for sensing applications is the split ring resonator (SRR). An SRR is a conductive ring structure with a gap cut out. These microwave structures have been applied extensively in the field of microwave sensing and have shown robust and highly accurate results for material characterization and sensing. The resonant mechanism of an SRR can be explained by Eq. 1, where its characteristic resonant frequency, f_{res}, is determined as a function of its length, L, wave velocity in vacuum, V_p, and the effective permittivity of the medium, ε_{eff} [49]. For a first-order mode resonance, Eq.1 requires the resonator length to be equal to half the wavelength ($L = \lambda/2$) [50].

$$f_{res} = \frac{V_p}{2L\sqrt{\varepsilon_{eff}}} \; [Hz]$$

SRRs implemented as microstrip structures can be excited with microstrip transmission lines that conventionally support quasi-TEM mode propagation. For ease of interpretation and design, such implementations require a model that can accurately predict the sensor response. The operation of such a microwave sensor can be modeled using a lumped-element equivalent circuit model. A circuit model of the presented sensor and its transmittance are observed in Fig. 2. The resonant behavior of such a microstrip line fed SRR can be monitored with respect to three variables: resonant frequency, f_{res}, resonant amplitude, A_{res}, and a -3dB or half-power quality factor, $QF_{-3dB} = f_{res}/f_h - f_L$.

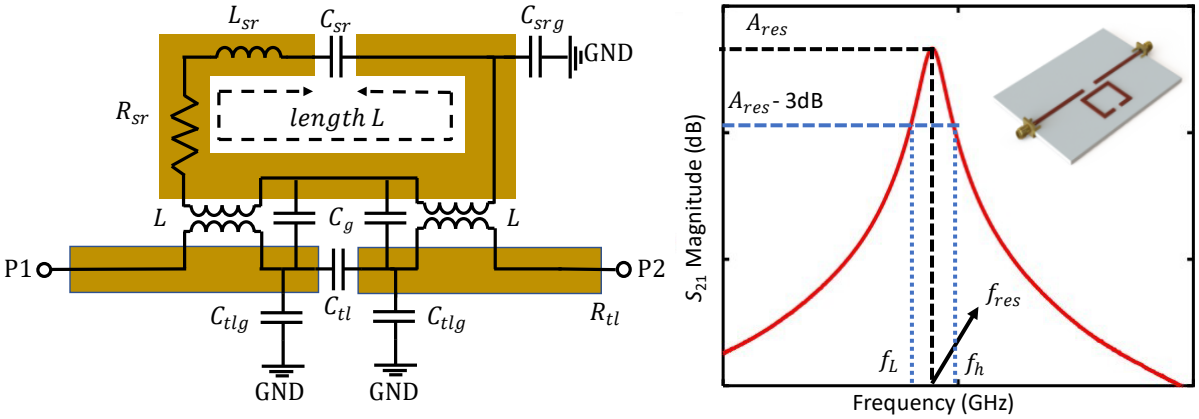

Figure 2: Split Ring Resonator (SRR) (a) depicted circuit model, (b) observed transmission gain (S_{21} (dB) response and parameters to monitor

This article has been accepted for publication in IEEE Microwave Magazine. This is the author's version which has not been fully edited and content may change prior to final publication. Citation information: DOI 10.1109/MMM.2023.3293617

The split region of a microwave resonator can be modeled as a capacitive region due to charge accumulation on the edges of the split. This capacitive section will result in a relatively high concentration of E-fields along the gap. Perturbation of the electric fields in this capacitive region can be regarded as a change in the effective permittivity (See Eq. 1), ε_{eff}, and results in a shift in the resonant characteristics, as seen in Fig. 3. The perturbation of field distributions can be modeled by changes in the capacitive element of an LC resonant circuit. Not only can different materials be characterized based on this change in resonant features, but also real-time changes in properties and the evolution of processes can be monitored. It is this unique property among various others that make such microwave sensors ideal for low power, conformal, real-time monitoring of ice/snow accretion and frost formation.

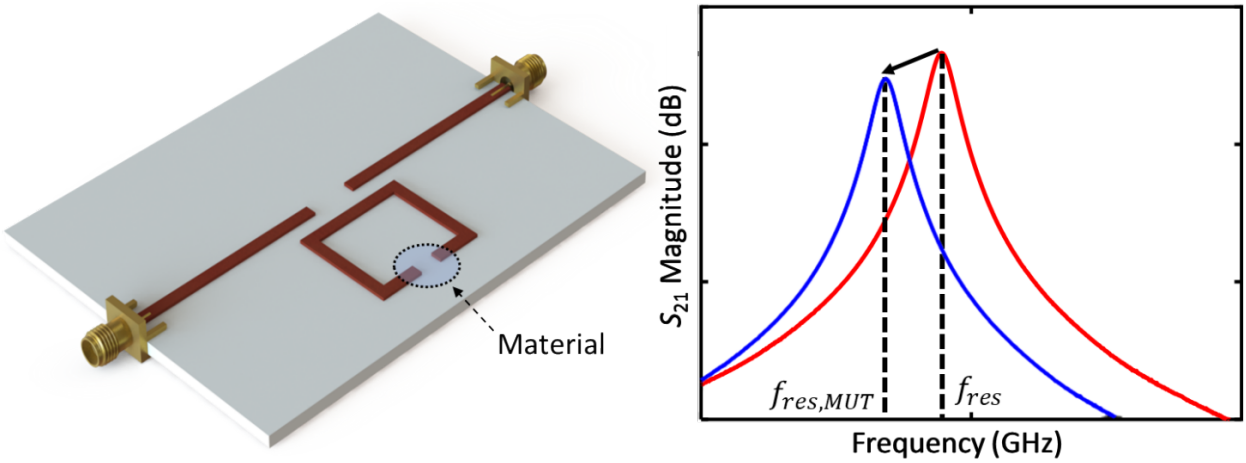

Figure 3: Split Ring Resonator (SRR) with (a) material placed on its sensitive gap, (b) change in transmission gain or S_{21} response of a sensor with application of material.

Electromagnetic Properties of Ice and Snow

Microwave measurement and characterization of ice, water, and snow have been thoroughly studied over the last century. Various methods of characterizing ice and snow as materials, defining parameters that describe their behavior, and extracting working models to predict them were applied. A comprehensive document, the "Engineering Properties of Ice and Snow", was published by Malcom Mellor in 1977 [51].

Ice and water each have distinct electromagnetic properties in the microwave regime. Considering these materials separately, we can obtain a dielectric permittivity and loss tangent value for each. Water has a real relative permittivity of 90 (at 0°C and 5GHz), and a very high loss tangent due to the water O-H bond polarization at microwave frequencies [52]. Ice has a dielectric permittivity of 3.2 (at 0°C and 5GHz) [52], [53]. This large difference in permittivity, as indicated in Fig.4, is very useful in clearly differentiating ice and water.

Ice accretion characteristics are far more complex and are determined based on local temperature, pressure, relative humidity, and water-ice mixtures. This results in ice formations with different densities, structures, and mixtures of ice, water, and air. Snow is a very good example of a mixture of ice, water and air where different environmental conditions affect its type and accretion characteristics. This makes ice and snow detection challenging, requiring thorough consideration for each variation of the material.

As microwave sensors detect material based on changes in effective permittivity, they can detect differences in accreted ice and snow based on densities and liquid water content [54], [55]. These relationships can be modeled using various microwave dielectric mixing theories [56]. In the field, empirical models can be used to obtain various characteristics of the snow depending on the frequency of operation and required accuracy. For frequencies between 10 MHz and 1 GHz, a first order approximation can be used to model the dielectric permittivity of accreted snow as a linear function of density, ρ, and a quadratic function of volumetric liquid water content W [55].

$$\varepsilon' = 1 + a\rho + bW + c\,W^2$$

Such simple models allow for easy characterization through the constants a, b, and c for different types and conditions of ice and snow depending on the sensing application. Using such empirical models, different environments at risk of dangerous accumulation of ice and snow, such as roadways, bridge cables, wind turbines, and airplanes, can be modeled and characterized.

This article has been accepted for publication in IEEE Microwave Magazine. This is the author's version which has not been fully edited and content may change prior to final publication. Citation information: DOI 10.1109/MMM.2023.3293617

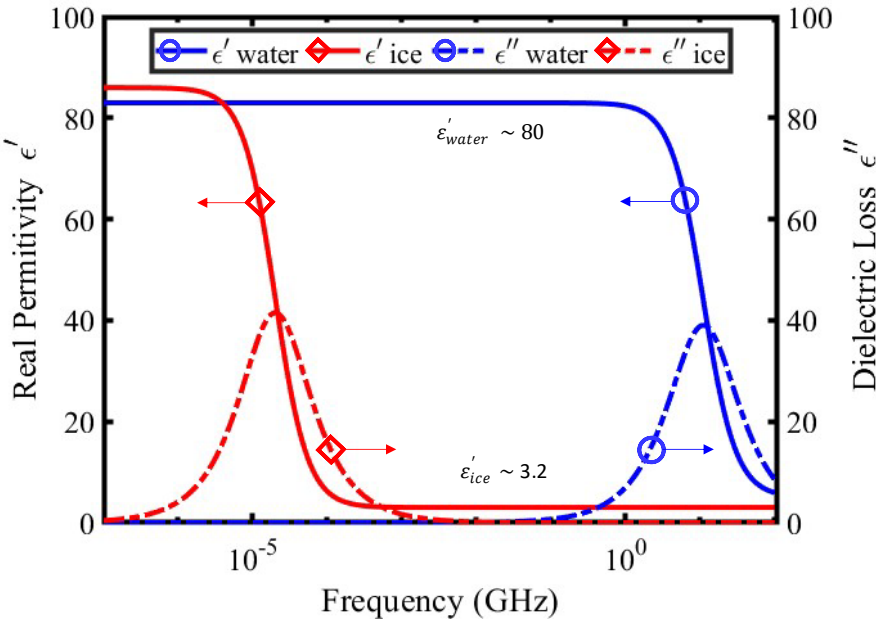

Figure 4: Real permittivity and dielectric loss of ice and water plotted against frequency.

Microwave Resonators for Ice Sensing

Microwave resonators can be geometrically tailored to function as a sensing element. These resonators can be implemented in a planar structure to provide a flat platform for ice buildup/accumulation. Microwave resonators can be incorporated into various topologies. Wiltshire et al. investigated SRRs for detecting ice formation on the split section and frost buildup on the entire surface of a passive sensor [57]. The sensor consisted of a double SRR structure that was electromagnetically coupled to two open-ended transmission lines. This component topology resulted in a band-pass frequency response of the passive sensor. This resonant structure had a resonant frequency of 4.85 GHz, a 3 dB quality factor of 250, and a peak S_{21} (dB) value of -14.5 dB. The sensitivity of the device's resonant response to frost formation was investigated by placing it on a Peltier device and cooling it to reach sub-zero temperatures (≈−10 °C) on the sensor's surface. The Peltier's temperature was controlled using a PID controller. The results of this investigation indicated that within only 15 secs of frost build-up, the entire resonant profile, including resonant frequency, resonant amplitude, and quality factor, changed with a noticeable trend as observed in Fig. 5. The formation of frost on the sensor changed the effective permittivity of the SRR's capacitive regions, ultimately changing the characteristics of the band-pass response. During the thawing process, with water (ε_r=80) on the resonator, the resonant quality factor was significantly degraded in the monitored frequency range since water's high permittivity substantially changed the effective permittivity in the resonator's nearby region. The split ring resonator's sensitivity to the effective permittivity of its nearby region was further confirmed by drop-casting a water droplet (ε_r=80) on the rings. Further icing of the droplet on the resonator was detected by monitoring the resonant profile over time as the sensor cooled. For droplet freezing, the sensor's resonant frequency had a of 220 MHz shift in the resonant frequency. The work presented by Wiltshire et al. showed the capability of microwave SRR sensors for monitoring ice, and frost formation, with the further ability of detecting transition states (i.e., ice to water and water to ice) in cold climatic conditions. Applying this technique, modified resonant structures have also been published for optimized ice thickness sensing [58].

This article has been accepted for publication in IEEE Microwave Magazine. This is the author's version which has not been fully edited and content may change prior to final publication. Citation information: DOI 10.1109/MMM.2023.3293617

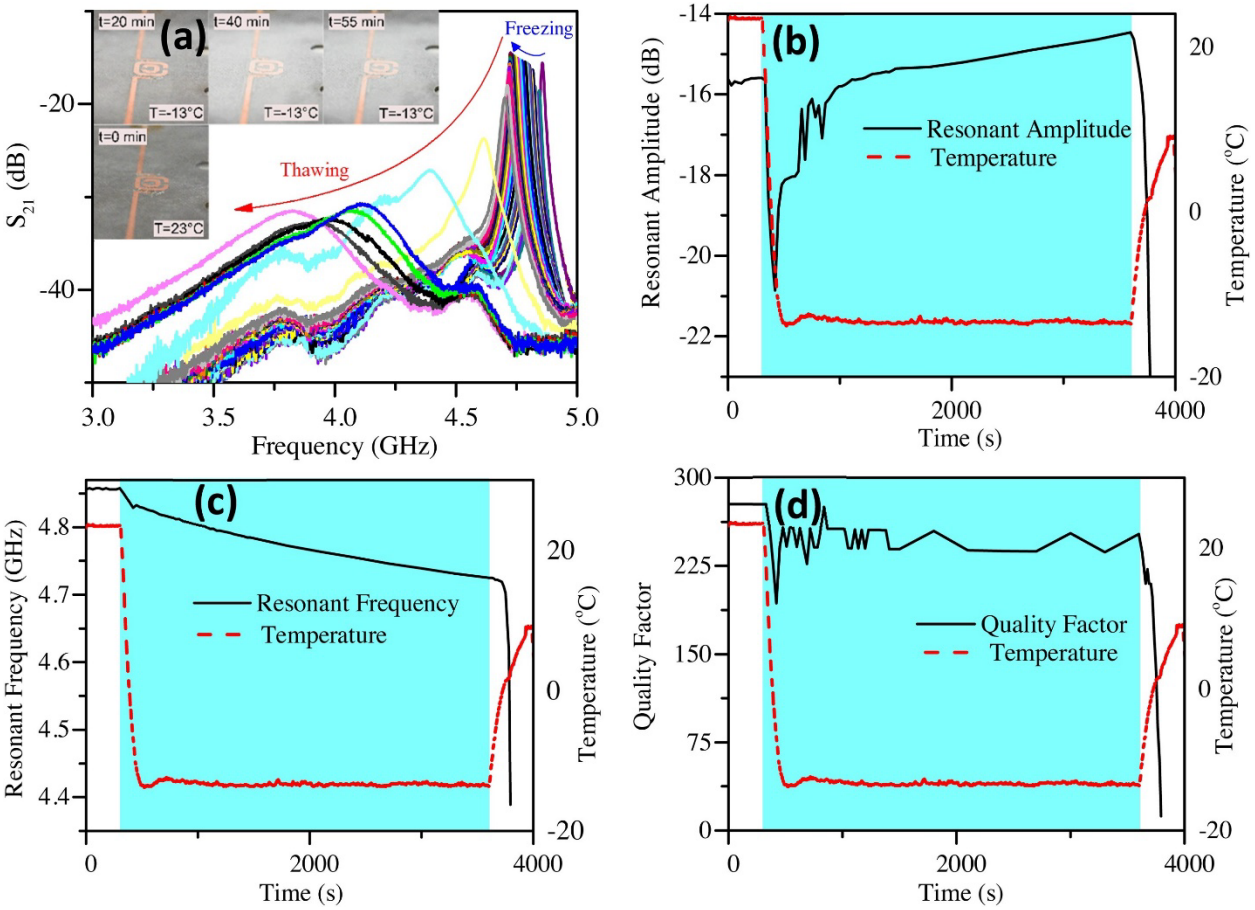

Figure 6: Frost formation on an SRR sensor. (a) time based S_{21} response of the freezing and thawing process, (b) resonant amplitude versus time, (c) resonant frequency versus time, and (d) quality factor versus time [57]

As mentioned earlier, the presence of water on the gap region of an SRR-based sensor can significantly decrease both the loaded and the un-loaded quality factor, which are monitorable in the bandpass response. This degradation in the quality factor was more pronounced when the dielectric loss factor of the water

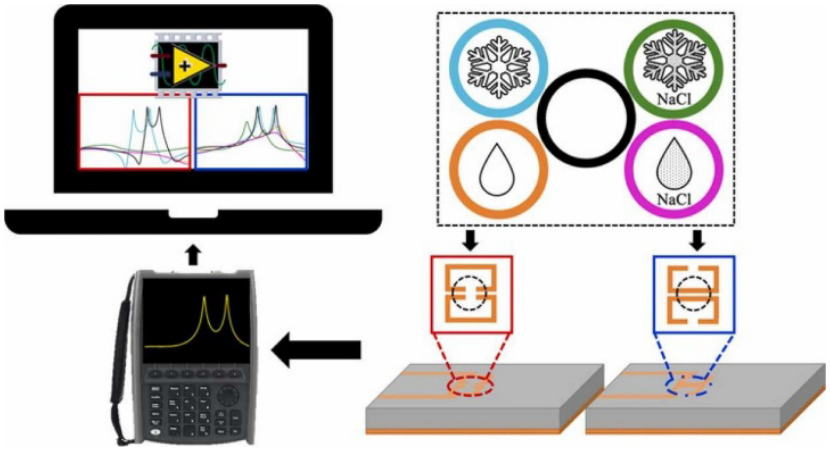

Figure 5: Salty ice detection based on modified coupling of SRR structures [59]

This article has been accepted for publication in IEEE Microwave Magazine. This is the author's version which has not been fully edited and content may change prior to final publication. Citation information: DOI 10.1109/MMM.2023.3293617

droplets increased. Such an increase can be attributed to the inclusion of conductive materials, most often salt and water mixture. The inclusion will remain after freezing (saline ice), and the loading effect of the salt-ice mixture will continue to degrade the bandpass resonant response. Consequently, a capacitance-dominant, split section of SRRs cannot be employed to monitor saline ice formation from salt water.

This issue was solved by Luckasavitch et al. [59], when they utilized the coupling mechanism between two SRRs to detect saline ice. By configuring the placement of the two SRRs, with their maximum current densities adjacent to each other, the dominant coupling mechanism occurred through magnetic fields. This configuration with the coupled SRR elements is shown in Fig. 7. This topology slightly reduced the sensitivity to permittivity variations in the coupled region, while introducing the capability of detecting conduction current variations for saline ice and water. For 80 µL of a 5% salt-water mixture, the coupled resonator sensor demonstrated a 119 MHz shift in resonant frequency upon ice formation. The results suggested that the "magnetically" coupled SRRs maintained the band-pass resonant profile necessary to distinguish saltwater and saline ice. This work, therefore, indicates that the coupling mechanism between adjacent resonators can be utilized to broaden the range of detectable materials, including but not limited to, saline ice and water.

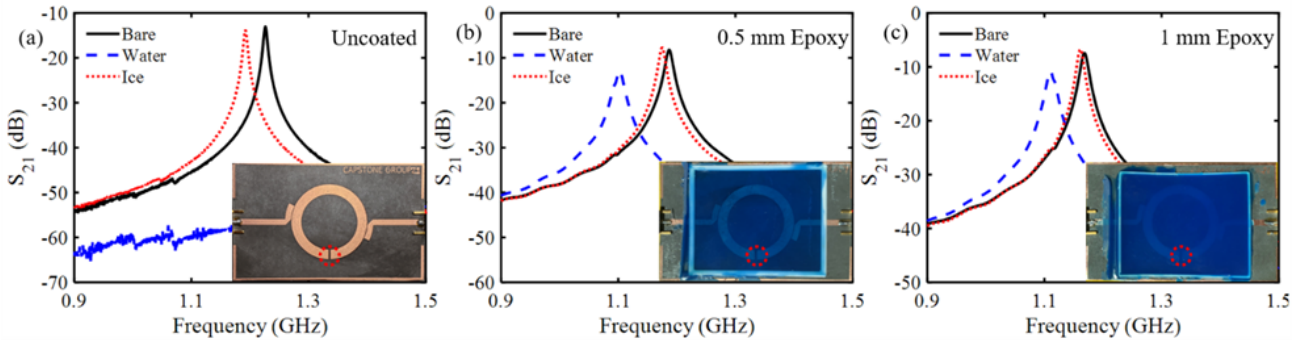

Figure 7: Measured bare, ice, and water response for the (a) uncoated, (b) 0.5 mm epoxy, and (c) 1 mm epoxy coated sensors. The red dotted circles indicate the placement of the material under test for each experiment. [60]

In real-world ice detection applications, it is common to apply coating layers to sensing instruments to increase their structural durability. Similarly, such coatings can be applied directly to the surface of a planar microwave sensor. It can be anticipated that a coating on the resonator might interfere with the operation of a planar microwave resonator sensor. To demonstrate the reliable functionality of a microwave sensor with an additional coating layer, Kozak et al. [60] developed an SRR-based (bandpass) ice sensor with protective (coated) epoxy on the surface of the resonator. This sensor comprised a circular split ring resonator operating at ~1.3 GHz, probed by two microstrip transmission lines that resulted in a loaded quality factor of 175. Fig. 7 demonstrates the SRR sensor with the protective epoxy covering the resonator surface. In this work, coating thicknesses of 0.5 mm and 1 mm were chosen and their effects on the resonant characteristics were studied. This sensor's resonant frequency shifted by 34, 12, and 6 MHz for ~50 µL of ice formed on the uncoated surface, on a 0.5 mm thick coating, and on a 1 mm thick coating, respectively. The coating layers with thicknesses of 0.5 mm and 1 mm on the surface of the resonator prevented the complete degradation of the band-pass response (within the monitored spectra) when water was present on the ring surface. By demonstrating resonator sensors functioning with a coating layer, this work showed the adaptability of microwave resonators to structural alteration and addition of materials.

Microwave resonator sensors based on microstrip transmission line excitation mechanisms have been shown to effectively detect ice, water, and salty ice, mimicking real-world scenarios. In addition, it has been demonstrated that the non-contact operation of microwave sensors can accommodate protective coating layers that improve their mechanical durability. Yet, for all the mentioned microwave resonator

This article has been accepted for publication in IEEE Microwave Magazine. This is the author's version which has not been fully edited and content may change prior to final publication. Citation information: DOI 10.1109/MMM.2023.3293617

sensors, the resonators are energized by transmission lines, which necessitate cabling to the resonator/sensor platform. In certain ice detection applications, the sensor can be exposed to harsh climatic conditions, and requirements like cabling and integrated electronic components may hinder sensor development. As a result, wireless methods of ice sensing are recommended for use in challenging environments.

Wireless Ice Sensing

The key motivation behind most microwave sensing approaches is to enable a seamless wireless readout of the measurands without the need for *additional* complex sensor-sampling circuitry [61]–[63]. Ice is a measurand which can be detected wirelessly in the far field through a change in the antenna's radiation properties and input impedance [61]. Like the planar resonator in Fig. 3, the effective permittivity of the medium surrounding the antenna will shift its resonance when an ice layer builds up. Given that ice is almost loss-less [52], the antenna's radiation efficiency can be maintained even in the presence of an ice layer [64].

Battery-Less RFID Sensors

The choice of the sensing antenna is dictated by the reading mechanism and the associated circuitry. For instance, UHF RFID dipoles have been widely applied in remote sensing applications [65]. The antennas in this case are tuned to the complex conjugate impedance of the RFID IC. Considering the permittivity of ice, should an ice "superstrate" build up on the antenna, a resonance shift and consequently a gain change are anticipated. In the lab, this can be differentially measured using a two-port VNA and a balanced common-ground jig [66], as shown in Fig. 8(a), for an antenna covered in ice. A key advantage of utilizing UHF RFID is that it significantly reduces the complexity of the wireless readout circuit and can be replaced by a handheld reader, as shown in Fig. 8(b), which can operate in harsh environments.

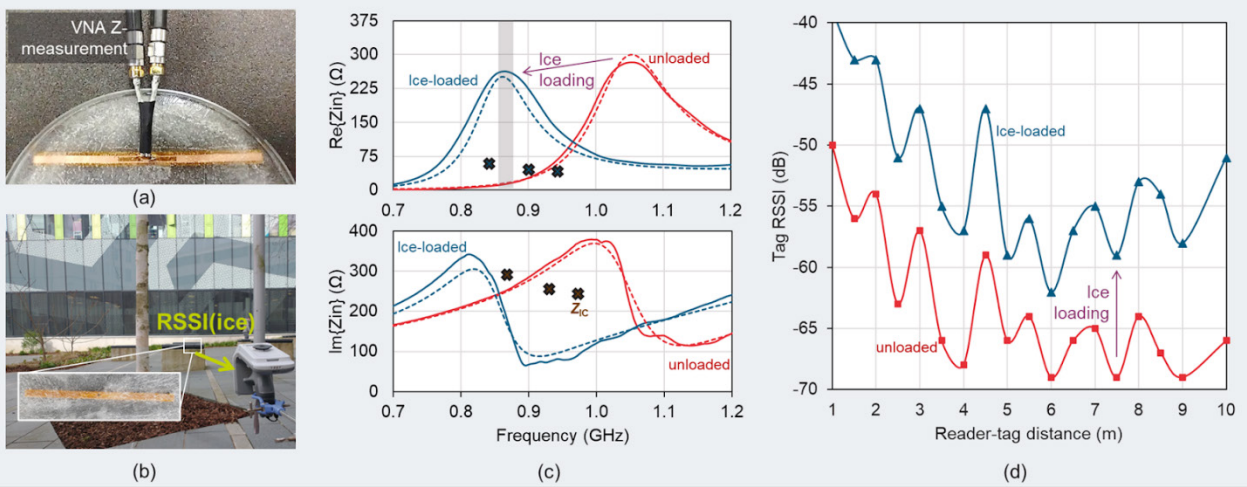

Figure 8: Battery-less positive-gain ice-sensing using RFID tags: (a) antenna impedance measurements with a soldered coaxial jig [66]*; (b) outdoor RSSI measurements; (c) measured (solid) and (dashed) impedance of the ice-loaded and unloaded RFID antenna showing the improved matching under loading; (d) the tag's measured RSSI before and after ice-loading showing up to 5 to 15 dB RSSI change.*[63]

Dipole-based complex-impedance RFID tag antennas have been proposed as long-range battery-free ice sensors with a very high accuracy in various deployment environments [63]. By tuning the antennas to resonate at a higher frequency f_0 than the frequency of interrogation f_r, the "detuning" effect introduced by the ice superstrate improves the matching of the tags, thus increasing the Received Signal Strength Indicator (RSSI). This concept of "positive sensing" is illustrated in Fig. 8(c), where the antenna's resonance shifts

toward the desired IC impedance when the ice builds up. This translates to an improved RSSI, as in Fig. 8(d); the large change, over +5 dB, in the RSSI enables the sensor to be read using any low-cost RFID reader. The thickness of the ice layer directly correlated with the frequency shift up to a certain point where the effect on the antenna's near-field plateaued. Moreover, given the large difference between the real permittivity of ice and water, see Fig. 4, a false match cannot be caused by the presence of water. To explain, water is highly lossy in the UHF spectrum, which degrades the antenna's gain, reducing the RSSI. Furthermore, the high permittivity will cause the resonance to shift to a lower frequency than f_r, leading to a further decay in the RSSI.

Antenna-Based Sensors

50 Ω-matched antennas were also investigated in ice-sensing applications. While the interaction of the antennas' near- and far-field with the ice layer will not, in principle, change based on the antenna's input impedance, the choice between a 50 Ω antenna and a complex-conjugate antenna will dictate the choice of the read-out circuit [61]. The advantage of 50 Ω antennas is their ability to integrate with commercial transceivers, voltage-controlled oscillators (VCOs) [60], and amplifiers or voltage detectors [67], enabling them to be a versatile platform for RF sensing. Similarly, they can be combined with an impedance matching network, which is insensitive to the ice layer, to match RFID ICs or rectennas [68]. Fig. 9 M2(a) illustrates an example sensing network that leverages 50 Ω antennas as the ice sensor.

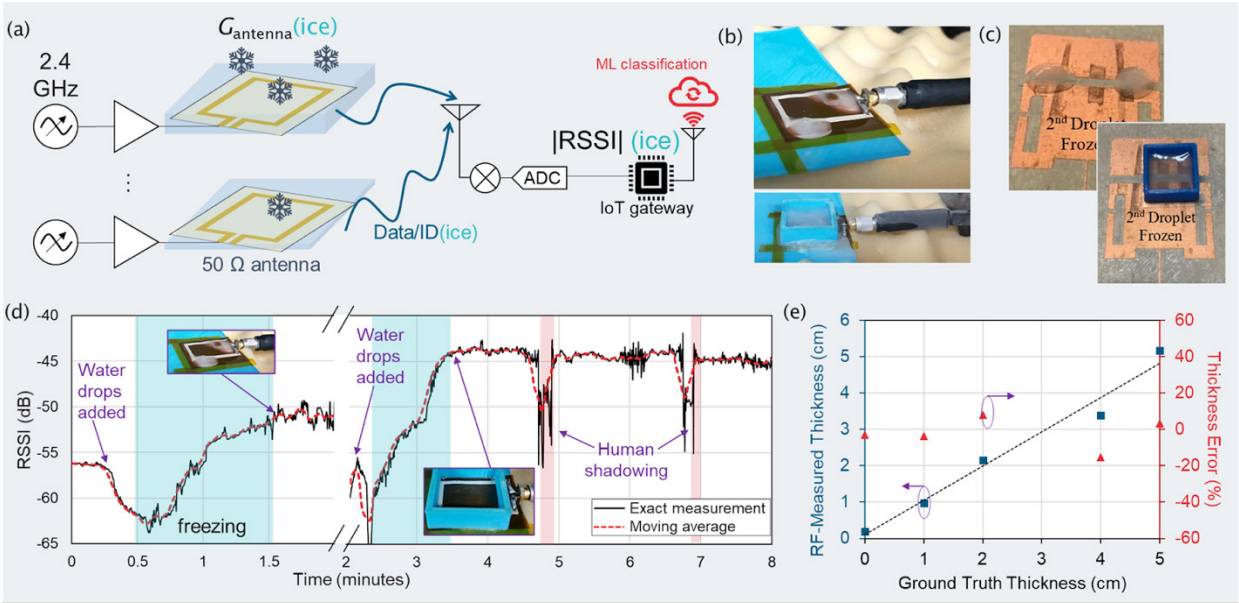

Figure 9:Wireless ice detection using 50 Ω-matched antennas: (a) example read-out circuit showing how multiple nodes could be read by a single gateway; (b) a flexible printed loop antenna designed for linearized gain-based sensing [61]*; (c) a miniaturized patch antenna utilizing a loading slot for ice sensing* [64]*; (d) time-varying far-field channel gain (RSSI) of the loop antenna inside a climatic chamber with added water droplets* [61]*; (e) wireless measurement of the ice thickness using the loop antenna based on the simulated ice-gain relation* [61].

Both aperture-type [64] and wire-type antennas [61] matched to 50 Ω have been used for wireless ice sensing. Wagih and Shi proposed the loop antenna shown in Fig 9 (b), fabricated using direct-write printing on a flexible substrate. The dimensions of the loop were optimized to maximize the sensitivity of the loop's resonance to the ice superstrate, which varies the capacitance and far-field radiation properties over the antenna's top plane. Kozak et al. proposed the patch shown in Fig. 9(c) which relied on T-slots to increase the sensitivity to small droplets of ice. For both antennas, the ice response manifested in the far-field gain,

which was measured in the lab environment using a two-port VNA; the S_{21} between the ice-sensing antenna and an insensitive reference was measured in the far-field. The S_{21} serves as an indicator of the expected RSSI value in a real-world setup. However, it is crucial to note that the receivers' resolution will limit that of the quantized RSSI.

In Fig. 9. (d), the real-time detection mechanism can be visualized following two freezing events. The sensing antenna was kept at -20°C and water droplets were added to emulate condensation on the antenna. Shortly after the water is added, the RSSI drops due to the increase in the water's imaginary permittivity as it cools, as shown in Fig. 4. The freezing event is then observed as soon as the RSSI starts rising. When the ice thickness increases, around minutes 2 to 4, a further increase in the RSSI is observed, which correlates to the expected increase in the gain as a result of improved matching under ice loading. This phenomenon was exploited to remotely quantify the thickness of the ice based on the antenna's gain change. As seen in Fig. 9(e), a thickness error below ±20% was observed. The ice-gain relation was obtained using the curve-fitted full-wave simulation results, and the sensor was tuned post-fabrication using a load of known dimensions [61].

Wagih and Shi extended the antenna design process to present a step-by-step methodology to designing a wireless antenna-based sensor [61] which can be summarized as:

1. Consider the practical limitations in terms of the available bandwidth, read-out circuit (discussed in the next section), and wireless range.
2. Choose the optimal RF parameter for sensing (i.e., the gain, S_{11}/S_{21}), as well as whether to measure the structure using the magnitude or the phase of the parameter under test.
3. Evaluate the linearity of the chosen parameter for varying ice thicknesses and iteratively optimize the parameter-under-test choice based on the electromagnetic simulations.

Targeting radome applications, standard geometry microstrip patch antennas were explored for ice sensing using their S_{11} magnitude [69]. While [69] used an antenna as the sensor, the sensor is not wireless, as the sensor's response is sampled at its input, through the S_{11}, as opposed to remotely, through the far-field properties. In a later implementation, a substrate with stable dielectric properties over temperature was chosen to ensure any resonance shifts observed were predominantly due to the ice and not the substrate's permittivity [76]. A similar study was performed in [61] showing that the variation in the permittivity of the antennas' substrate (Kapton) due to humidity changes was insignificant compared to the thickness of the ice.

Beyond the near-field interaction between the RFID antenna and the ice, the far-field channel response of RFID tags was also used to measure snow levels for environmental monitoring [70] or avalanche forecasting. The phase delay of a signal propagating through a thick layer of snow or ice could be used to extract information about the snowpack. This includes its density, moisture content, and any variation in the density of the accumulating layers. However, clearly differentiating the near-field "detuning" effects of the ice and snow building up on the tag from the additional phase delay in the channel requires further research to optimize the tags.

This article has been accepted for publication in IEEE Microwave Magazine. This is the author's version which has not been fully edited and content may change prior to final publication. Citation information: DOI 10.1109/MMM.2023.3293617

Passive Wireless Ice Detection

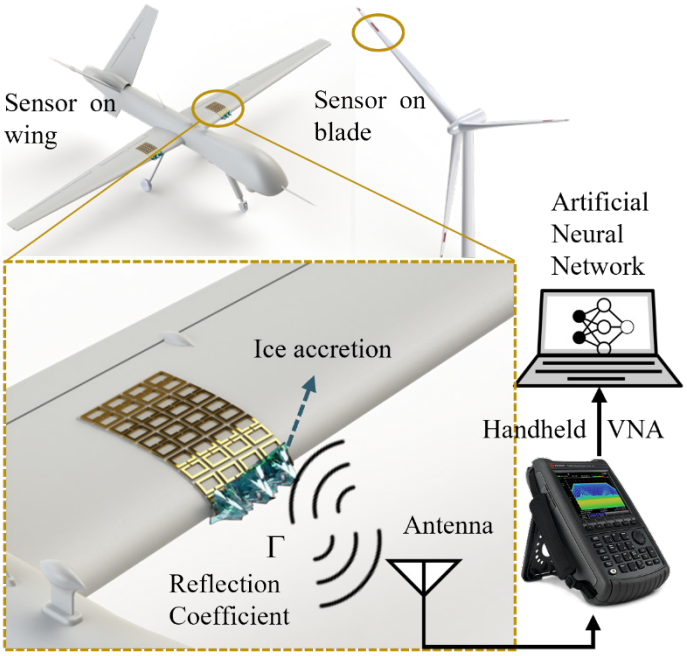

Figure 10: Passive wireless resonant tag for accurate chip-less sensing [71]

In order to avoid the need to integrate cabling, RFID chips, and batteries with the ice sensing platform, Niksan et al. demonstrated a fully passive frequency selective surface that was interrogated by an antenna for detecting ice and frost. An abstract representation of this process is depicted in Fig. 10. The frequency selective surface comprised 24 unit cells, uniformly arranged in an area of 13×6.5 cm^2, and monitoring was performed by interrogating the surface with a horn antenna [71]. Each frequency selecting unit cell consisted of a coupled arrangement of two standard split ring resonators. At resonant frequency, the designed array's surface impedance was matched to 377, resulting in a notch in the reflection coefficient of a normally incident plane wave. Yet, the presence of ice and water on the array altered the resonant characteristics of this surface, resulting in a sensitivity mechanism. This frequency selective array of SRRs, mounted on a substrate, was backed by a conductive material (copper) which effectively shielded the resonant characteristics from the effects of the background installation platform. It was shown that ~30 µL of water/ice droplets on the split section of the resonators caused a 150 MHz shift in the resonant frequency of this surface. In addition, when frost formed on the surface as a result of a temperature drop, there was a 19 MHz shift in the resonance frequency. This work highlighted the versatility of microwave ice sensing in a variety of installation circumstances, as a resonant surface sensitive to ice and frost formation was developed that did not require any cable connections or RFID chips (and batteries) attached to the sensing platform.

This article has been accepted for publication in IEEE Microwave Magazine. This is the author's version which has not been fully edited and content may change prior to final publication. Citation information: DOI 10.1109/MMM.2023.3293617

Readout Circuit for Microwave Ice Sensing

Planar and wireless microwave sensors have demonstrated the ability to detect ice and frost accretion. For implementation in real-world environments, bulky and expensive vector network analyzers must be replaced. To achieve this a portable readout circuit was demonstrated by Kozak et.al to detect and differentiate ice through 0.5 mm of protective coating. The schematic of the readout circuit is shown in Fig. 11(a) and the fabricated readout circuit is shown in Fig. 11(b). The readout circuit consisted of a voltage-controlled oscillator (ZX95-1480-S+ from Mini-Circuits) tuned to generate a signal at 1.17 GHz, which excited the SRR. A wideband power detector (ZX47-40LN-S+ from Mini-Circuits) was used to convert the high-frequency output signal from the SRR sensor into a measurable DC signal. The power detector's output was subtracted from a DC reference voltage using a differential amplifier and was further amplified using a tunable non-inverting amplifier to achieve maximum dynamic range while avoiding saturation. The read-out circuit was tuned to have an output of -3.586 V in the presence of ice and 1.359 V in an unloaded state [60]. The power detector's output DC voltage can then be passed to a microcontroller such as an ESP32 or an Arduino Nano to determine the sensor's status (presence or absence of ice and water) and to transfer this information to a remote base station or smart phone via wired or wireless communication. This work highlighted the ease with which a microwave sensor can be integrated with a portable and wireless readout system capable of monitoring the formation of ice in real time. The readout system can be further integrated with systems and algorithms to lower the impact of noise and temperature variation on readout telemetry performance.

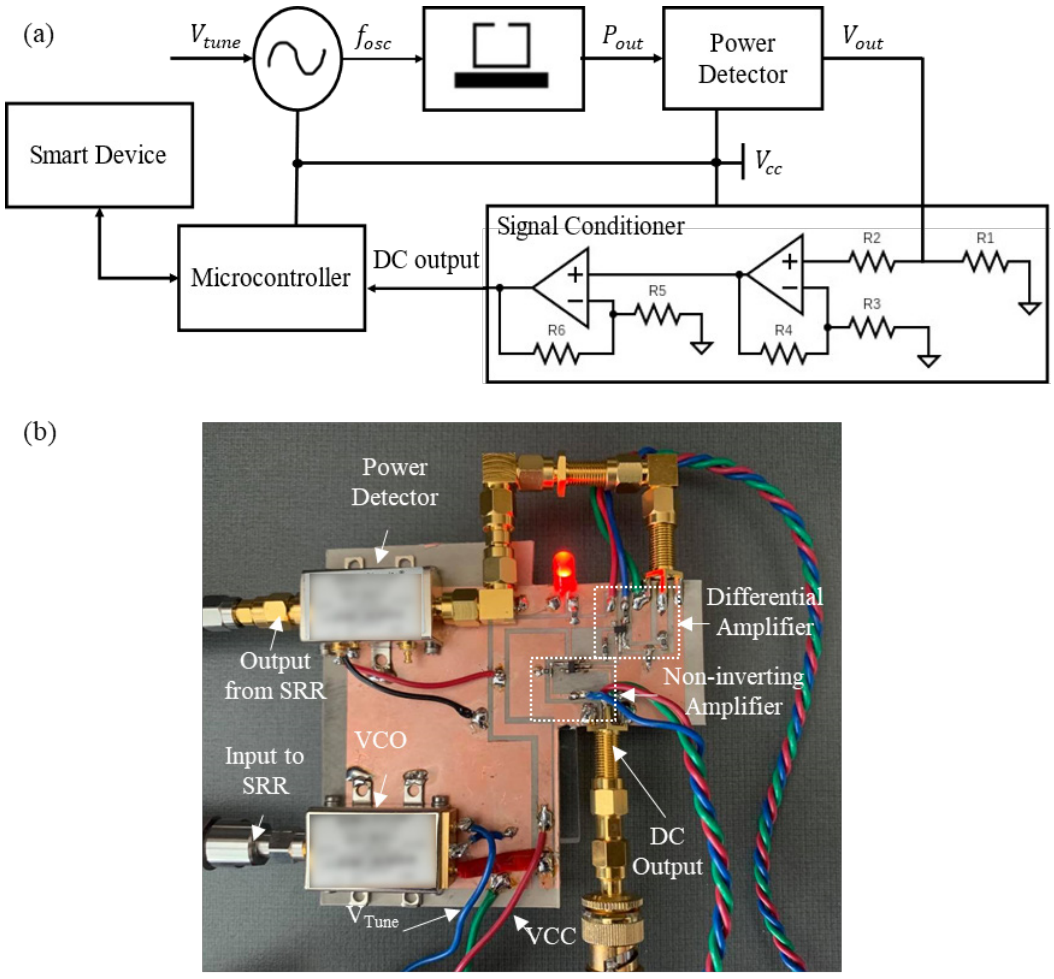

Figure 11: (a) Schematic of a readout circuit to detect ice and water on an SRR sensor using a VCO, power detector, and microcontroller, and (b) fabricated readout circuit. [60]

This article has been accepted for publication in IEEE Microwave Magazine. This is the author's version which has not been fully edited and content may change prior to final publication. Citation information: DOI 10.1109/MMM.2023.3293617

Machine Learning Applied

In non-ideal environments, readout telemetry performance can degrade rapidly as noise and temperature variations cause jumps, non-linear responses, and discontinuities in the data. Recently, Artificial Neural Networks (ANN) and machine learning models have gained significant attention in microwave engineering due to their ability to solve complex problems and are being applied for real time compensation in decision making [72]. Kazemi et al. produced two solutions to the problem of temperature variation causing erroneous measurements in microwave sensors by applying an ANN to accurately detect various liquids under a variety of temperatures [73][74]. Niksan et al. demonstrated post-processing advancements by incorporating an artificial neural network for ice detection [71]. The artificial neural network differentiated the microwave array's three test conditions of bare, ice, and water to a high accuracy of 96.49% in stable conditions. However, due to the proposed wireless method of sensing, an artificial neural network was employed to compensate for outside noise, temperature variation, and signal interference. The ANN was tested under various noise conditions in increments of 5% signal interference with the associated confusion matrix for 5% interference shown in Fig. 12. The trained ANN successfully identified the test responses with an accuracy of 93.33% up to 5% interference while deteriorating to 62% accuracy at an extreme of 20% interference. Because of the success and ongoing advancements of artificial neural networks, examples such as Niksan et al. can now be embedded into smartphone apps to create fully remote, reliable, and automated detection systems in the palm of your hand.

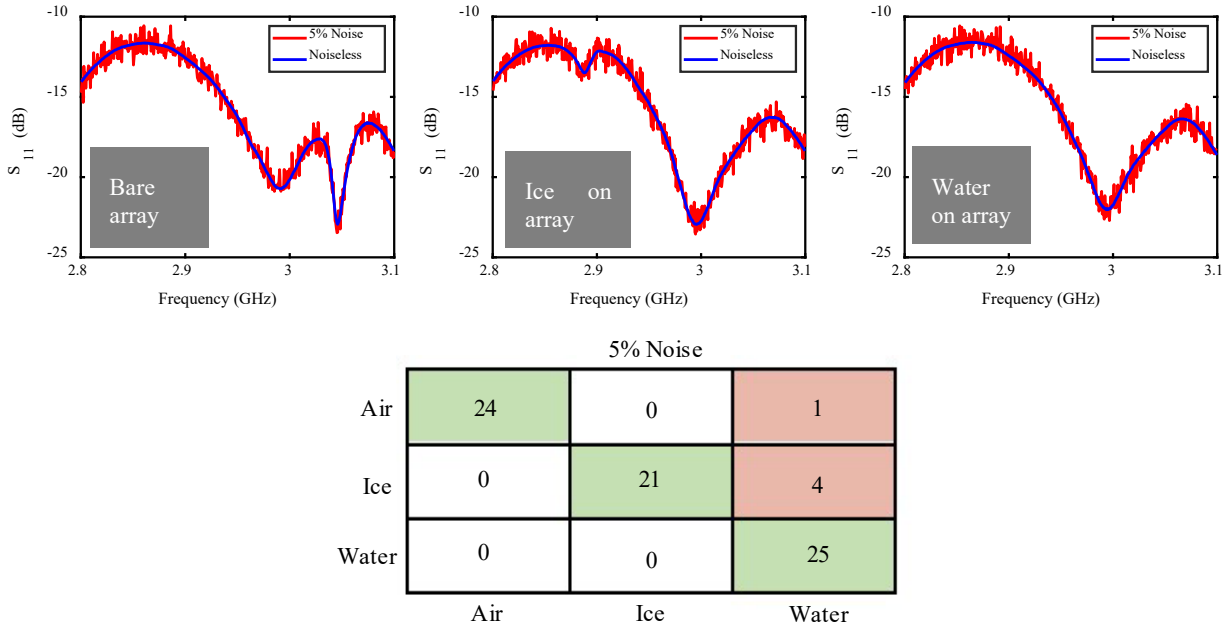

Figure 12: (a) Simulated response with 5% additive noise for all three test cases (b) ANN's associated confusion matrix for 5% of incremental noise [71]

This article has been accepted for publication in IEEE Microwave Magazine. This is the author's version which has not been fully edited and content may change prior to final publication. Citation information: DOI 10.1109/MMM.2023.3293617

Encapsulation, Materials, and Packaging

Microwave ice sensors would typically operate outdoors in a harsh environment. Therefore, proper packaging is key to ensure that the sensors' lifetime matches that of the surface they are attached to (e.g., wind turbines). In some of the reported systems, RFICs, such as packaged commercial RFID ICs [62], [63], were used. More complex systems using an S-parameter (S_{11}) readout circuit based on a voltage control oscillator (VCO), couplers, and detectors have also been reported. The complexity of these readout circuits makes it necessary to consider not only size, cost, and power consumption, but also the mechanical reliability and ability to conform to the deployment surface.

A conformable vacuum-forming coating process using thin polyimide (Kapton) films was used in [63] to waterproof the ice-sensing RFID dipoles and to improve the mechanical reliability of the tags. This packaging technique was originally proposed for textile-integrated machine-washable RFID tags and flexible circuit filaments and has been shown to withstand over 30 washing cycles [63]. The advantage of UHF "Gen-2" RFID sensors is an increased mechanical reliability, as well as a flexible and conformable form-factor very similar to its chipless counterpart [71]. A model of this novel encapsulation method is

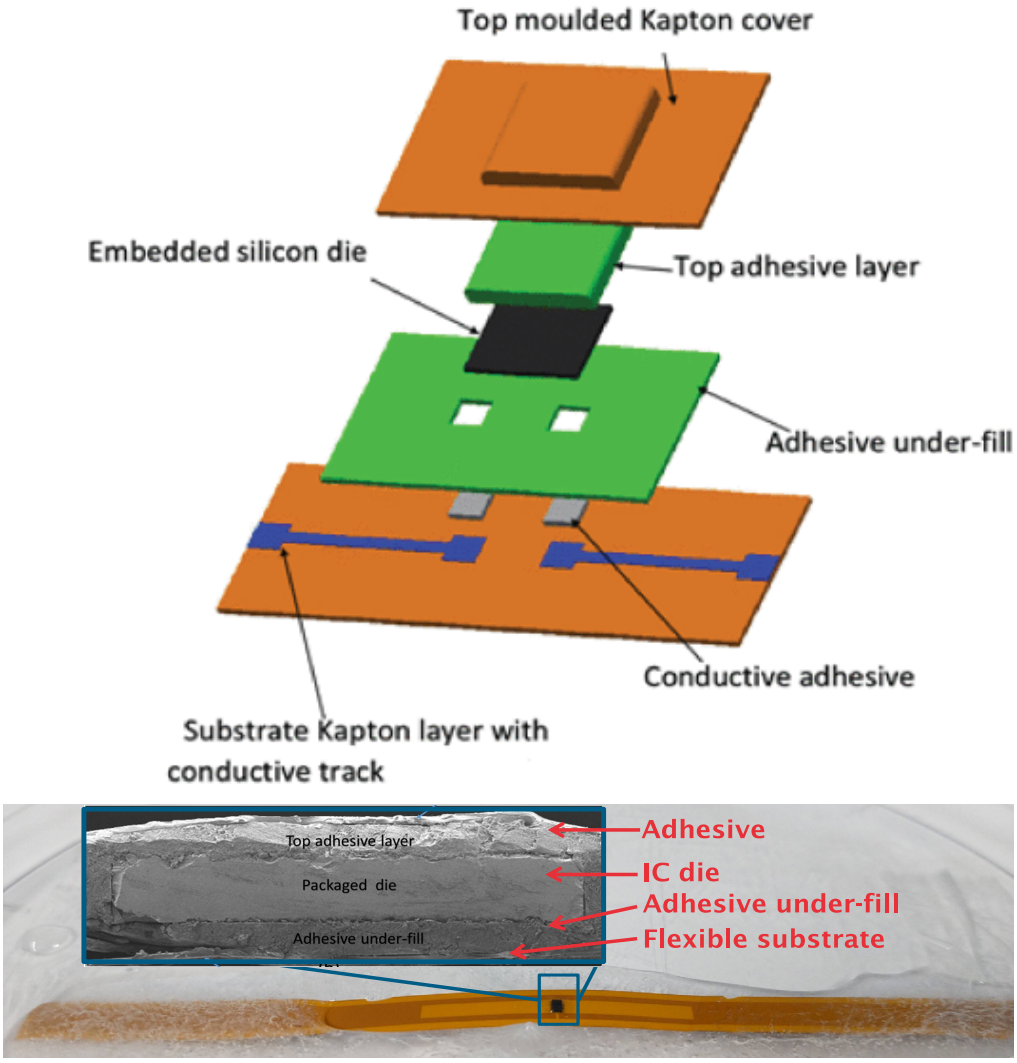

Figure 13: Novel multilayer packaging of IC chips on flexible substrates [63]

presented in Fig. 13. The fabricated sensor and a cross-section of the IC protection on the sensor is also displayed.

To protect PCB-based resonant microwave ice sensors, epoxy coatings of varying thicknesses were investigated in [60]. The epoxy loading varied both the resonant frequency and the Q-factor of a two-port resonator, owing to the high E-field density in the epoxy layer. However, thin epoxy coatings have little effect on the Q-factor and the sensor can still be read reliably. Chipless planar and conformable PCB sensors are expected to have the highest mechanical and environmental reliability and stability [71]. This is because, the absence of discrete rigid ICs reduces the mechanical forces on the components and all-passive planar structures have a higher resilience to bending and mechanical stress [75].

Integrated Ice-Sensing Solutions

Integrated Electrothermal De-icing

Sensing ice is only part of the challenge with ice and snow. After ice is detected, a system must begin applying de-icing measures. Electrothermal de-icing is a modern method of de-icing applied in various applications like airplanes, wind turbines, and driveways. Kozak et al. presented a planar SRR resonator sensor with embedded resistive heating within the microstrip ground plane in [76].

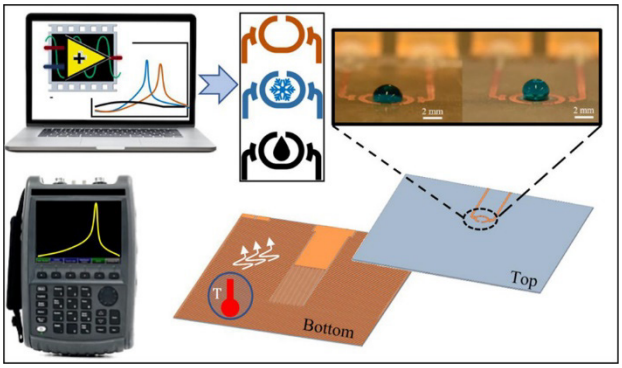

Figure 14: Superhydrophobic coated modified microwave sensor with a patterned ground heater for detection and prevention of ice accumulation. [76] Reprinted with permission from R. Kozak, B. D. Wiltshire, Md. A. R. Khandoker, K. Golovin, and M. H. Zarifi, "Modified Microwave Sensor with a Patterned Ground Heater for Detection and Prevention of Ice Accumulation," ACS Applied Materials & Interfaces, vol. 12, no. 49, pp. 55483–55492, Nov. 2020, doi: https://doi.org/10.1021/acsami.0c17173.. Copyright 2020 American Chemical Society.

The planar structure of the SRR sensor further allows the additional functionality of "heating" for the prevention of ice accumulation. Compared to conventional SRR structures, this work replaced the intact ground plane with patterned traces to increase the DC resistance of the ground plane to effectively utilize it as a heater.

Coatings for De-icing

Furthermore, the planar topology of the SRR sensor allowed the application of an ice-phobic coating on its surface to investigate the effectiveness of such engineered materials. Kozak et al. investigated the freezing rates of droplets on superhydrophobic treated and untreated SRRs. The treated surface was able to delay freezing time by 250s, which is equivalent to a decrease in the freezing rate by a factor of three. Moreover, by fitting the melting curves and extracting the time constants of heated and unheated sensors, it was found that the heating decreased the normal melting time by a factor of two. This work demonstrated the overall multi-functionality of an SRR-based sensing structure and the ability to incorporate de-icing and anti-icing capabilities into a single sensor device.

Integrated System

This article has been accepted for publication in IEEE Microwave Magazine. This is the author's version which has not been fully edited and content may change prior to final publication. Citation information: DOI 10.1109/MMM.2023.3293617

Azimi Dijvejin et al. demonstrate an integrated smart, hybrid (passive and active) de-icing system through the combination of low interfacial toughness (LIT) coatings, printed circuit board heaters, and an ice-detecting microwave sensor in [77]. Upon sensing ice and snow with the installed microwave sensor, the integrated system applies minimal heating to induce crack propagation and subsequent de-icing at low temperatures and forces without melting the ice (shown in Fig. 15).

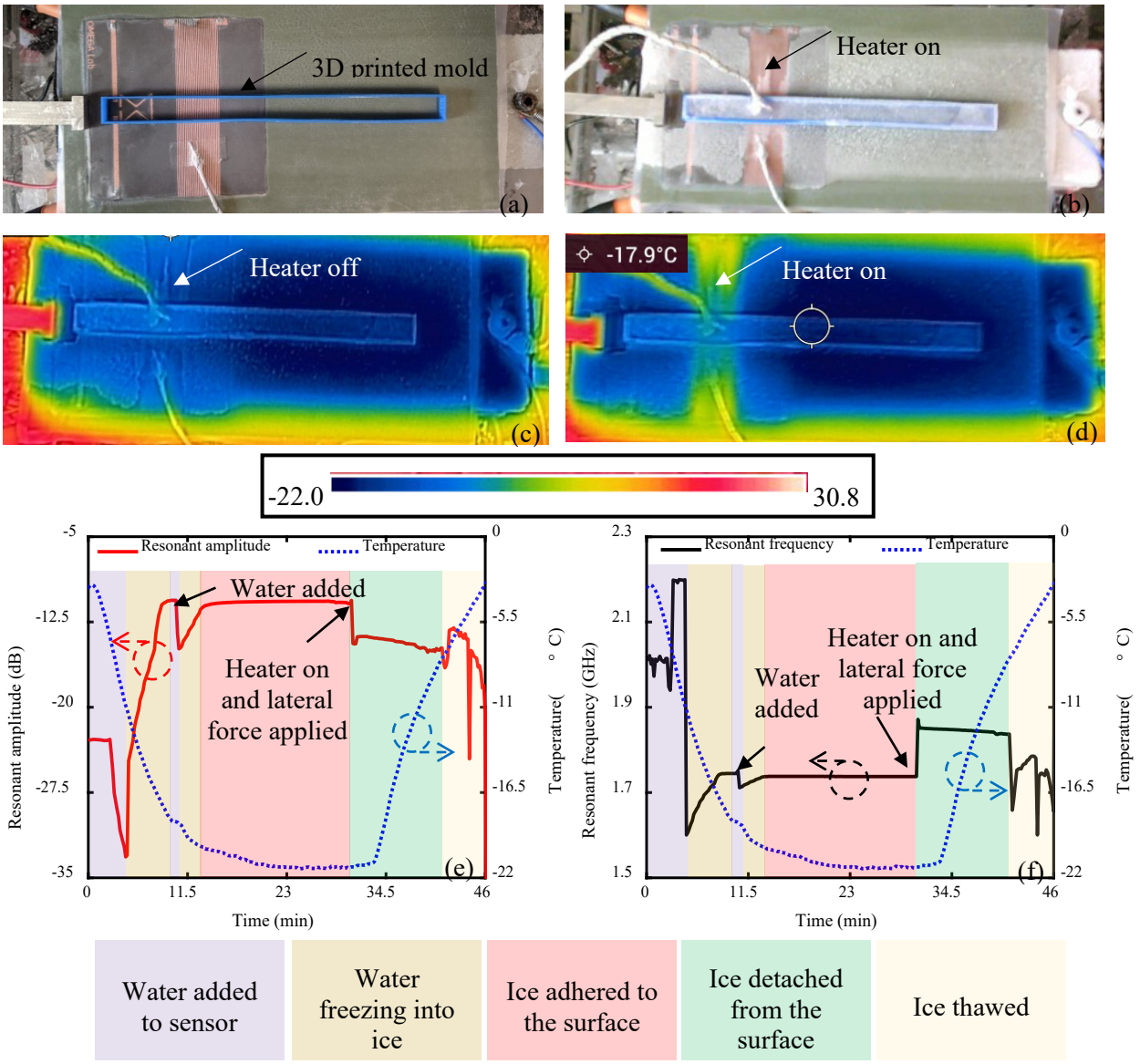

Figure 15: (a) Prototype panel on a Peltier stage with a 3D printed mold for ice testing. (b) ice with embedded thermocouple frozen on the prototype panel. Infrared images showing the heat map of the prototype panel (c) before switching on the heater and (d) after switching on the heater. (e) Recorded resonant amplitude and (f) resonant frequency vs. time depicting the water being frozen to the LIT coating covering the sensor, heating the surface locally from -21°C to -5°C, detaching the ice at -5°C with a shear force, and then thawing the system. [77]

This low-power integrated system, which applies materials technology and integrated sensing and heating capabilities for de-icing, is a clear step toward the next phase of localized, optimized ice sensing and de-icing.

Conclusion

Microwave sensors have demonstrated highly accurate measurement of frost formation and ice and snow accretion. Ice and snow are complex mixtures that display different behaviors based on different real-world ambient conditions. Microwave sensors offer accurate ways of measuring the various parameters of interest from the accreted mixture and can be used for future optimization of integrated localized ice sensing and de-icing systems.

These sensors offer real time sensing of the monitored accretion location from under protective and de-icing coatings. The low-cost fabrication and conformal implementation of these devices make them ideal for applications that range from roadway de-icing to airplane and wind turbine monitoring. The versatility of these sensors allows for operation as low-power wireless sensors, with considerations for coatings and environmental conditions surrounding the sensing challenge. For real-world deployment, microwave-based ice sensors can be scaled to be compatible with wireless communication standards and protocols like Bluetooth, Zigbee, and LoRa. The complexity of the readout circuitry can be minimized through large scale integration in CMOS technology for extremely low power consumption and a miniaturized form factor. By combining such sensors with machine learning algorithms and material models, powerful smart-sensor devices can be implemented in the harshest of environments.

Various projects to design microwave ice sensors for roadways, airplanes, and wind turbines are currently underway and this patented technology [78] is expected to pave the way toward wireless, integrated ice sensing and de-icing systems of tomorrow.

References

[1] P. Przyborski and R. Levy, "Snow Cover," *EOS Project Science Office, NASA Goddard Space Flight Center*, Feb. 01, 2022. https://earthobservatory.nasa.gov/global-maps/MOD10C1_M_SNOW (accessed Nov. 05, 2022).

[2] E. Kim, "How Can We Find Out How Much Snow Is in the World?," *Eos (Washington DC)*, vol. 99, Jun. 2018, doi: 10.1029/2018EO099939.

[3] Federal Highway Administration (FHWA), "Snow & Ice," *Road Weather Management*, Jul. 26, 2022. https://ops.fhwa.dot.gov/weather/weather_events/snow_ice.htm (accessed Nov. 05, 2022).

[4] M. Farzaneh, Ed., *Atmospheric Icing of Power Networks*. Dordrecht: Springer Netherlands, 2008. doi: 10.1007/978-1-4020-8531-4.

[5] M. Virk, M. Mustafa, and Q.-A. Hamdan, "Atmospheric Ice Accretion Measurement Techniques," *Int J Multiphys*, vol. 5, no. 3, pp. 229–242, Sep. 2011, doi: 10.1260/1750-9548.5.3.229.

[6] T. Rashid, H. A. Khawaja, and K. Edvardsen, "Review of marine icing and anti-/de-icing systems," *Journal of Marine Engineering & Technology*, vol. 15, no. 2, pp. 79–87, May 2016, doi: 10.1080/20464177.2016.1216734.

[7] H. Hu, "The science behind frozen wind turbines – and how to keep them spinning through the winter," *The Conversation*, Mar. 04, 2021. https://theconversation.com/the-science-behind-frozen-wind-turbines-and-how-to-keep-them-spinning-through-the-winter-156520 (accessed Nov. 05, 2022).

[8] D. G. Jackson and J. I. Goldberg, "Ice Detection Systems: A Historical Perspective," Sep. 2007. doi: 10.4271/2007-01-3325.

[9] K. Petty and C. Floyd, "A statistical review of aviation airframe icing accidents in the U.S," in *11th Conference on Aviation, Range, and Aerospace*, Oct. 2004. Accessed: Nov. 05, 2022. [Online]. Available: https://www.researchgate.net/publication/287186718_A_statistical_review_of_aviation_airframe_icing_accidents_in_the_US

[10] U. N. Mughal, M. S. Virk, and M. Y. Mustafa, "State of the Art Review of Atmospheric Icing Sensors," *Sensors & Transducers*, vol. 198, no. 3, pp. 2–15, 2016, Accessed: Nov. 05, 2022. [Online]. Available: https://www.proquest.com/docview/1781331985?pq-origsite=gscholar&fromopenview=true

[11] P. J. Jordaens *et al.*, "Available Technologies for Wind Energy in Cold Climates," in *IEA Wind Task 19*, May 2016. Accessed: Nov. 05, 2022. [Online]. Available: https://www.researchgate.net/publication/305881044_IEA_Wind_Task_19_-_Available_Technologies_report_of_Wind_Energy_in_Cold_Climates

[12] AC-9C Aircraft Icing Technology Committee, "Minimum Operational Performance Specification for Inflight Icing Detection Systems." SAE International, Apr. 2022. doi: https://doi.org/10.4271/AS5498B.

[13] AC-9C Aircraft Icing Technology Committee, "Aircraft Inflight Ice Detectors and Icing Rate Measuring Instruments." SAE International, May 2022. doi: https://doi.org/10.4271/AIR4367B.

[14] Collins Aerospace, "Primary & advisory ice detection systems," 2019. Accessed: Nov. 06, 2022. [Online]. Available: https://prd-sc101-cdn.rtx.com/-/media/ca/product-assets/marketing/i/ice-detection/primary-and-advisory-ice-detection-systems.pdf

[15] T. Schlegl, M. Moser, and H. Zangl, "Wireless and Flexible Ice Detection on Aircraft," in *SAE Technical Papers*, Jun. 2015, vol. 2015-June, no. June. doi: 10.4271/2015-01-2112.

[16] "ON Wing Ice DetectioN and MonitorinG System Reporting Project Information Final Report Summary-ON-WINGS (On wing ice detection and monitoring system)."

[17] "All-in-one Optical Sensor for Advanced Ice Detection," 2020. Accessed: Nov. 05, 2022. [Online]. Available: https://www.collinsaerospace.com/-/media/CA/product-assets/marketing/o/optical-ice-detector-data-sheet.pdf

[18] D. Fuleki, Z. Sun, J. Wu, and G. Miller, "Development of a non-intrusive ultrasound ice accretion sensor to detect and quantify ice accretion severity," in *9th AIAA Atmospheric and Space Environments Conference, 2017*, 2017. doi: 10.2514/6.2017-4247.

[19] Y. Liu, L. J. Bond, and H. Hu, "Ultrasonic-attenuation-based technique for ice characterization pertinent to aircraft icing phenomena," *AIAA Journal*, vol. 55, no. 5, pp. 1602–1609, 2017, doi: 10.2514/1.J055500.

[20] A. Piccardi and L. Colace, "Optical Detection of Dangerous Road Conditions.," *Sensors (Basel)*, vol. 19, no. 6, Mar. 2019, doi: 10.3390/s19061360.

[21] J. Ge, L. Ye, and J. Zou, "A novel fiber-optic ice sensor capable of identifying ice type accurately," *Sens Actuators A Phys*, vol. 175, pp. 35–42, Mar. 2012, doi: 10.1016/j.sna.2011.12.016.

[22] Tekmar, "Installation & Operation Manual," 2016.

[23] M. H. Zarifi *et al.*, "A microwave ring resonator sensor for early detection of breaches in pipeline coatings," *IEEE Transactions on Industrial Electronics*, vol. 65, no. 2, pp. 1626–1635, Jul. 2017, doi: 10.1109/TIE.2017.2733449.

[24] O. Krivosudský, D. Havelka, D. E. Chafai, and M. Cifra, "Microfluidic on-chip microwave sensing of the self-assembly state of tubulin," *Sens Actuators B Chem*, vol. 328, p. 129068, Feb. 2021, doi: 10.1016/J.SNB.2020.129068.

[25] J. Munoz-Enano, O. Peytral-Rieu, P. Velez, D. Dubuc, K. Grenier, and F. Martin, "Characterization of the Denaturation of Bovine Serum Albumin (BSA) Protein by Means of a Differential-Mode Microwave Microfluidic Sensor Based on Slot Resonators," *IEEE Sens J*, vol. 22, no. 14, pp. 14075–14083, Jul. 2022, doi: 10.1109/JSEN.2022.3181542.

[26] Y. Kozhemyakin, S. Rehault-Godbert, D. Dubuc, and K. Grenier, "Millifluidic Sensor Designed to Perform the Microwave Dielectric Spectroscopy of Biological Liquids," *2022 52nd European Microwave Conference (EuMC)*, pp. 1–4, Sep. 2022, doi: 10.23919/EUMC54642.2022.9924355.

[27] A. Ebrahimi, W. Withayachumnankul, S. Al-Sarawi, and D. Abbott, "High-sensitivity metamaterial-inspired sensor for microfluidic dielectric characterization," *IEEE Sens J*, vol. 14, no. 5, pp. 1345–1351, 2014, doi: 10.1109/JSEN.2013.2295312.

[28] M. Abdolrazzaghi, M. H. Zarifi, and M. Daneshmand, "Wireless Communication in Feedback-Assisted Active Sensors," *IEEE Sens J*, vol. 16, no. 22, pp. 8151–8157, Nov. 2016, doi: 10.1109/JSEN.2016.2604855.

[29] B. D. Wiltshire, T. Zarifi, and M. H. Zarifi, "Passive Split Ring Resonator Tag Configuration for RFID-Based Wireless Permittivity Sensing," *IEEE Sens J*, vol. 20, no. 4, pp. 1904–1911, Feb. 2020, doi: 10.1109/JSEN.2019.2950912.

[30] F. Martin, "Introduction to Planar Microwave Sensors," in *Planar Microwave Sensors*, Wiley, 2022, pp. 1–64. doi: 10.1002/9781119811060.ch1.

[31] O. Niksan, M. C. Jain, A. Shah, and M. H. Zarifi, "A Nonintrusive Flow Rate Sensor Based on Microwave Split-Ring Resonators and Thermal Modulation," *IEEE Trans Microw Theory Tech*, vol. 70, no. 3, 2022, doi: 10.1109/TMTT.2022.3142038.

[32] M. Mallach, P. Gebhardt, and T. Musch, "2D microwave tomography system for imaging of multiphase flows in metal pipes," *Flow Measurement and Instrumentation*, vol. 53, pp. 80–88, Mar. 2017, doi: 10.1016/J.FLOWMEASINST.2016.04.002.

[33] J. Muñoz-Enano, P. Vélez, M. Gil, and F. Martín, "Planar Microwave Resonant Sensors: A Review and Recent Developments," *Applied Sciences 2020, Vol. 10, Page 2615*, vol. 10, no. 7, p. 2615, Apr. 2020, doi: 10.3390/APP10072615.

[34] Aquar System Industrial Solutions, "A444 microwave consistency sensor," 2020. https://aquar-system.com/measurements/consistency/a444/ (accessed Nov. 06, 2022).

[35] E. G. Nyfors and A. Wee, "Measurement of mixtures of oil, water, and gas with microwave sensors: new developments and field experience of the MFI MultiPhase and WaterCut meters of Roxar," *https://doi.org/10.1117/12.390612*, vol. 4129, pp. 12–21, Jul. 2000, doi: 10.1117/12.390612.

[36] "Roxar | Emerson CA." https://www.emerson.com/en-ca/automation/roxar (accessed Nov. 06, 2022).

[37] S. Guha, F. I. Jamal, and C. Wenger, "A Review on Passive and Integrated Near-Field Microwave Biosensors," *Biosensors 2017, Vol. 7, Page 42*, vol. 7, no. 4, p. 42, Sep. 2017, doi: 10.3390/BIOS7040042.

[38] M. E. Peters, D. D. Blankenship, and D. L. Morse, "Analysis techniques for coherent airborne radar sounding: Application to West Antarctic ice streams," *J Geophys Res Solid Earth*, vol. 110, no. B6, pp. 1–17, Jun. 2005, doi: 10.1029/2004JB003222.

[39] J. Waters, "Chemistry of the Atmosphere: Observations for Chemistry (Remote Sensing): Microwave," *Encyclopedia of Atmospheric Sciences: Second Edition*, pp. 418–428, 2015, doi: 10.1016/B978-0-12-382225-3.00271-1.

[40] V. v. Tikhonov, M. D. Raev, E. A. Sharkov, D. A. Boyarskii, I. A. Repina, and N. Y. Komarova, "Satellite microwave radiometry of sea ice of polar regions: a review," *Izvestiya, Atmospheric and Oceanic Physics 2016 52:9*, vol. 52, no. 9, pp. 1012–1030, Feb. 2017, doi: 10.1134/S0001433816090267.

[41] J. F. Galantowicz and J. Picton, "Flood Mapping with Passive Microwave Remote Sensing: Current Capabilities and Directions for Future Development," *Earth Observation for Flood Applications: Progress and Perspectives*, pp. 39–60, Jan. 2021, doi: 10.1016/B978-0-12-819412-6.00003-1.

[42] C. T. Swift, D. C. Dehority, A. B. Tanner, and R. E. McIntosh, "PASSIVE MICROWAVE SPECTRAL EMISSION FROM SALINE ICE AT C-BAND DURING THE GROWTH PHASE.," *IEEE Transactions on Geoscience and Remote Sensing*, vol. GE-24, no. 6, Nov. 1985, doi: 10.1109/TGRS.1986.289698.

[43] S. Mousavi, R. D. de Roo, K. Sarabandi, A. W. England, S. Y. E. Wong, and H. Nejati, "Lake Icepack and Dry Snowpack Thickness Measurement Using Wideband Autocorrelation Radiometry," *IEEE Transactions on Geoscience and Remote Sensing*, vol. 56, no. 3, pp. 1637–1651, Mar. 2018, doi: 10.1109/TGRS.2017.2765924.

[44] A. K. Jha, N. K. Tiwari, and M. J. Akhtar, "Accurate microwave cavity sensing technique for dielectric testing of arbitrary length samples," *IEEE Trans Instrum Meas*, vol. 70, Apr. 2021, doi: 10.1109/TIM.2021.3073438.

[45] R. Ramzan, O. Siddiqui, M. Omar, and O. M. Ramahi, "Energy Tunneling: A Way to Achieve Highly Sensitive Material Detection with Sub-Wavelength Resolution," *IEEE Microw Mag*, vol. 20, no. 11, pp. 32–48, Nov. 2019, doi: 10.1109/MMM.2019.2935390.

[46] M. Fayaz, M. H. Zarifi, M. Abdolrazzaghi, P. Shariaty, Z. Hashisho, and M. Daneshmand, "A Novel Technique for Determining the Adsorption Capacity and Breakthrough Time of Adsorbents Using a Noncontact High-Resolution Microwave Resonator Sensor," *Environ Sci Technol*, vol. 51, no. 1, pp. 427–435, Jan. 2017, doi: 10.1021/ACS.EST.6B03418/ASSET/IMAGES/MEDIUM/ES-2016-03418Y_0009.GIF.

[47] A. Mason *et al.*, "Noninvasive In-Situ measurement of blood Lactate using microwave sensors," *IEEE Trans Biomed Eng*, vol. 65, no. 3, pp. 698–705, Mar. 2018, doi: 10.1109/TBME.2017.2715071.

[48] A. K. Jha, N. K. Tiwari, and M. Jaleel Akhtar, "Novel microwave resonant technique for accurate testing of magnetic materials," *IEEE Trans Microw Theory Tech*, vol. 67, no. 1, pp. 239–248, Jan. 2019, doi: 10.1109/TMTT.2018.2880964.

[49] J. D. Baena *et al.*, "Equivalent-circuit models for split-ring resonators and complementary split-ring resonators coupled to planar transmission lines," *IEEE Trans Microw Theory Tech*, vol. 53, no. 4 II, pp. 1451–1460, Apr. 2005, doi: 10.1109/TMTT.2005.845211.

[50] D. M. Pozar, *Microwave Engineering, 4th Edition*. Wiley, 2012. Accessed: Nov. 06, 2022. [Online]. Available: https://www.wiley.com/en-ca/Microwave+Engineering%2C+4th+Edition-p-9780470631553

[51] M. Mellor, "Engineering Properties of Snow," *Journal of Glaciology*, vol. 19, no. 81, 1977, [Online]. Available: https://www.cambridge.org/core.

[52] V. G. Artemov, "A unified mechanism for ice and water electrical conductivity from direct current to terahertz," *Physical Chemistry Chemical Physics*, vol. 21, no. 15, pp. 8067–8072, Apr. 2019, doi: 10.1039/C9CP00257J.

[53] M. E. Tiuri, A. H. Sihvola, E. G. Nyfors, and M. T. Hallikaiken, "The Complex Dielectric Constant of Snow at Microwave Frequencies," *IEEE Journal of Oceanic Engineering*, vol. 9, no. 5, pp. 377–382, 1984, doi: 10.1109/JOE.1984.1145645.

[54] W. I. Linlor, "Permittivity and attenuation of wet snow between 4 and 12 GHz," *J Appl Phys*, vol. 51, no. 5, pp. 2811–2816, 1980, doi: 10.1063/1.327947.

[55] A. Denoth *et al.*, "A comparative study of instruments for measuring the liquid water content of snow," *Journal of Applied Physics*, vol. 56, no. 7. pp. 2154–2160, 1984. doi: 10.1063/1.334215.

[56] W. R. Tinga, W. A. G. Voss, and D. F. Blossey, "Generalized approach to multiphase dielectric mixture theory," *J Appl Phys*, vol. 44, no. 9, pp. 3897–3902, 1973, doi: 10.1063/1.1662868.

[57] B. Wiltshire, K. Mirshahidi, K. Golovin, and M. H. Zarifi, "Robust and sensitive frost and ice detection via planar microwave resonator sensor," *Sens Actuators B Chem*, vol. 301, p. 126881, Dec. 2019, doi: 10.1016/J.SNB.2019.126881.

[58] J. Xie, J. Wen, J. Chen, and W. Yuan, "Microwave Icing Sensor Based on Interdigital-Complementary Split-Ring Resonator," *IEEE Sens J*, vol. 22, no. 13, pp. 12829–12837, Jul. 2022, doi: 10.1109/JSEN.2022.3176932.

[59] K. Luckasavitch, R. Kozak, K. Golovin, and M. H. Zarifi, "Magnetically coupled planar microwave resonators for real-time saltwater ice detection," *Sens Actuators A Phys*, vol. 333, p. 113245, Jan. 2022, doi: 10.1016/J.SNA.2021.113245.

[60] R. Kozak, M. C. Jain, J. McClelland, A. Shah, and M. Zarifi, "Durable Ice Sensors utilizing Microwave SRRs Coated with Protective Epoxy for De-Icing Control," in *Proceedings of IEEE Sensors*, 2021, vol. 2021-October. doi: 10.1109/SENSORS47087.2021.9639610.

[61] M. Wagih and J. Shi, "Toward the Optimal Antenna-Based Wireless Sensing Strategy: An Ice Sensing Case Study," *IEEE Open Journal of Antennas and Propagation*, vol. 3, pp. 687–699, 2022, doi: 10.1109/OJAP.2022.3182770.

[62] M. Wagih and J. Shi, "Complex-Impedance Dipole Antennas as RFID-Enabled Ice Monitors," in *2021 IEEE International Symposium on Antennas and Propagation and North American Radio Science Meeting, APS/URSI 2021 - Proceedings*, 2021, pp. 399–400. doi: 10.1109/APS/URSI47566.2021.9704082.

[63] M. Wagih and J. Shi, "Wireless Ice Detection and Monitoring Using Flexible UHF RFID Tags," *IEEE Sens J*, vol. 21, no. 17, pp. 18715–18724, Sep. 2021, doi: 10.1109/JSEN.2021.3087326.

[64] R. Kozak, K. Khorsand, T. Zarifi, K. Golovin, and M. H. Zarifi, "Patch antenna sensor for wireless ice and frost detection," *Sci Rep*, vol. 11, no. 1, Dec. 2021, doi: 10.1038/s41598-021-93082-2.

[65] G. Marrocco, "RFID Grids: Part I—Electromagnetic Theory," *IEEE Trans Antennas Propag*, vol. 59, no. 3, pp. 1019–1026, Mar. 2011, doi: 10.1109/TAP.2010.2103019.

[66] K. D. Palmer and M. W. vanRooyen, "Simple Broadband Measurements of Balanced Loads Using a Network Analyzer," *IEEE Trans Instrum Meas*, vol. 55, no. 1, pp. 266–272, Feb. 2006, doi: 10.1109/TIM.2005.861493.

[67] C. Li, T. Djerafi, E. Villeneuve, and K. Wu, "Planar antenna sensor with thermal stability for detection of ice formation," *Sens Actuators A Phys*, vol. 341, p. 113576, Jul. 2022, doi: 10.1016/j.sna.2022.113576.

[68] M. Wagih, A. S. Weddell, and S. Beeby, "Rectennas for Radio-Frequency Energy Harvesting and Wireless Power Transfer: A Review of Antenna Design [Antenna Applications Corner]," *IEEE Antennas Propag Mag*, vol. 62, no. 5, pp. 95–107, Oct. 2020, doi: 10.1109/MAP.2020.3012872.

[69] R. U. Tariq, M. Ye, X.-L. Zhao, S.-C. Zhang, Z. Cao, and Y.-N. He, "Microwave Sensor for Detection of Ice Accretion on Base Station Antenna Radome," *IEEE Sens J*, vol. 21, no. 17, pp. 18733–18741, Sep. 2021, doi: 10.1109/JSEN.2021.3089320.

[70] M. le Breton, É. Larose, L. Baillet, Y. Lejeune, and van Herwijnen, "Monitoring snowpack SWE and temperature using RFID tags as wireless sensors," *EGUsphere [preprint]*, 2022.

[71] O. Niksan, K. Colegrave, and M. H. Zarifi, "Battery-Free, Artificial Neural Network-Assisted Microwave Resonator Array for Ice Detection," *IEEE Trans Microw Theory Tech*, vol. 71, no. 2, pp. 698–709, 2023, doi: 10.1109/TMTT.2022.3222194.

[72] K. Colegrave, M. C. Jain, O. Niksan, and M. Zarifi, "Artificial Neural Networks for Antenna-based Contactless Liquid Classification," in *2022 International Conference on Electrical, Computer and Energy Technologies (ICECET)*, 2022, pp. 1–5. doi: 10.1109/ICECET55527.2022.9872637.

[73] N. Kazemi, M. Abdolrazzaghi, and P. Musilek, "Comparative Analysis of Machine Learning Techniques for Temperature Compensation in Microwave Sensors," *IEEE Trans Microw Theory Tech*, vol. 69, no. 9, pp. 4223–4236, Sep. 2021, doi: 10.1109/TMTT.2021.3081119.

[74] N. Kazemi, M. Abdolrazzaghi, P. Musilek, and M. Daneshmand, "A Temperature-Compensated High-Resolution Microwave Sensor Using Artificial Neural Network," *IEEE Microwave and Wireless Components Letters*, vol. 30, no. 9, pp. 919–922, Sep. 2020, doi: 10.1109/LMWC.2020.3012388.

[75] M. Wagih, A. Komolafe, and N. Hillier, "Screen-Printable Flexible Textile-Based Ultra-Broadband Millimeter-Wave DC-Blocking Transmission Lines Based on Microstrip-Embedded Printed Capacitors," *IEEE Journal of Microwaves*, vol. 2, no. 1, pp. 162–173, Jan. 2022, doi: 10.1109/JMW.2021.3126927.

[76] R. Kozak, B. D. Wiltshire, M. A. R. Khandoker, K. Golovin, and M. H. Zarifi, "Modified Microwave Sensor with a Patterned Ground Heater for Detection and Prevention of Ice Accumulation," *ACS Appl Mater Interfaces*, vol. 12, no. 49, pp. 55483–55492, Dec. 2020, doi: 10.1021/acsami.0c17173.

[77] Z. Azimi Dijvejin, M. C. Jain, R. Kozak, M. H. Zarifi, and K. Golovin, "Smart low interfacial toughness coatings for on-demand de-icing without melting," *Nat Commun*, vol. 13, no. 1, p. 5119, Aug. 2022, doi: 10.1038/s41467-022-32852-6.

[78] K. Golvin, M. Zarifi, B. Wiltshire, K. Mirshahidi, and R. Kozak, "Method and apparatus for detecting ice formation on a surface using resonant sensors," Jul. 23, 2020

This article has been accepted for publication in IEEE Microwave Magazine. This is the author's version which has not been fully edited and content may change prior to final publication. Citation information: DOI 10.1109/MMM.2023.3293617